

Two dimensional images of dissolved sulphide and metals in anoxic sediments by a novel DGTprobe and optical scanning techniques

Gao, Yue; Van De Velde, Sebastiaan; Williams, P.; Baeyens, Willy; Zhang, Hao

Published in:
TrAC. Trends in Analytical Chemistry

DOI:
[10.1016/j.trac.2014.11.012](https://doi.org/10.1016/j.trac.2014.11.012)

Publication date:
2015

Document Version:
Submitted manuscript

[Link to publication](#)

Citation for published version (APA):
Gao, Y., Van De Velde, S., Williams, P., Baeyens, W., & Zhang, H. (2015). Two dimensional images of dissolved sulphide and metals in anoxic sediments by a novel DGTprobe and optical scanning techniques. *TrAC. Trends in Analytical Chemistry*, 66, 63-71. <https://doi.org/10.1016/j.trac.2014.11.012>

Copyright

No part of this publication may be reproduced or transmitted in any form, without the prior written permission of the author(s) or other rights holders to whom publication rights have been transferred, unless permitted by a license attached to the publication (a Creative Commons license or other), or unless exceptions to copyright law apply.

Take down policy

If you believe that this document infringes your copyright or other rights, please contact openaccess@vub.be, with details of the nature of the infringement. We will investigate the claim and if justified, we will take the appropriate steps.

Two dimensional images of dissolved sulphide and metals in anoxic sediments by a novel DGT probe and optical scanning techniques

Yue Gao ^{1,#}

Sebastiaan van de Velde ¹

Paul N. Williams ^{2,3}

Willy Baeyens ¹

Hao Zhang ²

¹ Analytical, Environmental and Geo-Chemistry (AMGC), Faculty of Science, Vrije Universiteit Brussel, Pleinlaan 2, Brussels, Belgium

² Lancaster Environmental Centre, Lancaster University, Lancaster LA1 4YQ, UK

³ Insititute for Global Food Security, Queen's University Belfast, Belfast BT9 5HN, UK

Corresponding author: yuegao@vub.ac.be (Tel. +32 2 629 32 61)

Submitted to: Trends in Analytical Chemistry

Keywords: DGT, 2D image, trace metal, dissolved sulphide, remobilisation, LA-ICP-MS

Version: final

NOTICE: this is the author's version of a work that was accepted for publication in Trends in Analytical Chemistry. Changes resulting from the publishing process, such as peer review, editing, corrections, structural formatting, and other quality control mechanisms may not be reflected in this document. Changes may have been made to this work since it was submitted for publication. A definitive version was subsequently published in Trends in Analytical Chemistry, 66(2015) 63-71, DOI 10.1016/j.trac.2014.11.012

1 **ABSTRACT**

2 A novel Diffusive Gradients in Thin Film (DGT) probe is developed consisting of a
3 diffusive AgI gel layer and a back-up microchelex resin gel layer. 2D high resolution images
4 of sulphide and trace metals were determined respectively on the AgI gel by densitometric
5 analysis and on the microchelex resin layer with Laser Ablation (LA)-ICPMS.

6 The validity of the analytical procedures used for the determination of sulphide and trace
7 metals has been investigated: low RSDs on replicate measurements, linear trace metal
8 calibration curves between the LA-ICP-MS signal and the true trace metal concentration in
9 the resin gel and a good agreement of the sulphide results obtained with the AgI resin gel and
10 with other analytical methods were found.

11 The method was applied on anoxic sediment pore waters in an estuarine and a marine
12 system. Simultaneous remobilisation of sulphide and trace metals was observed in the marine
13 sediment.
14

1 1. INTRODUCTION

2 Diagenetic processes control the geochemical behaviour of trace metals in contaminated
3 lacustrine and marine sediments. They are the result of the oxidation of organic matter by a
4 suite of oxidants whereby O₂ will be first consumed and then successively NO₃⁻, Mn⁴⁺,
5 Fe³⁺ and SO₄²⁻ and induce changes in redox potential and pH as well as in the levels of
6 sulphide, carbonate and organic matter. These changes affect the trace metal speciation for
7 example their immobilisation by dissolved sulphide but also their re-dissolution by a decrease
8 of the pH or an increase of the redox potential and their release back to the water column
9 thereby threatening the ecosystem.

10 To understand these complex processes, geochemists need information about the spatial
11 distribution of the trace metals and of the most important parameters influencing that
12 distribution. In anoxic sediments, dissolved sulphide is without any doubt the most important
13 parameter that controls the trace metal distribution [1, 2]. Therefore in this paper we will
14 focus on the analytical tools available to determine the spatial distributions of trace metals and
15 sulphide in anoxic sediment pore waters. Redox potential and pH distributions are also very
16 important but they are determined by different, electrochemical methods [3, 4].

17 Initially, undisturbed sediment cores were sampled and then sliced and centrifuged in a
18 flow hood under nitrogen to assess vertical profiles of trace metal and sulphide concentrations
19 [5, 6]. There are at least three major constraints with this procedure: (1) the analyses of the
20 very low concentrations of the trace metals and the sulphide require relatively large pore
21 water volumes; (2) but even with more sensitive techniques, the slicing of the sediment cores
22 is nevertheless limited to about 0.5 cm and (3) the slightest introduction of air during the
23 treatment of the sediment in the flow hood jeopardizes the results. A much better solution is
24 to use the passive sampler technique of Diffusive Gradients in Thin Films (DGT), a kinetic
25 regime passive sampler, because it allows a much higher spatial resolution and it is an in situ
26 technique, eliminating the risk of contamination during sample treatment [7, 8].

27 The rectangular DGT probe used in sediments is 180 mm x 40 mm, with a window of 150
28 x 18 mm open to sediments and consisting of two hydrogel layers: mostly a polyacrylamide
29 gel covered with a membrane (0.45 µm) is used as the diffusive layer, and is backed up by a
30 second thin gel layer containing an AgI resin gel for dissolved sulphide and a Chelex cation-
31 exchange resin (100 µm bead size) selective for metals. With this technique, only the labile
32 metal and sulphide fractions, small enough to diffuse through the diffusive gel and capable of
33 binding to the resin layer are assessed. After deployment, the Chelex resin gel is sliced into 5

1 mm strips and the metals are eluted with 1M HNO₃ solution, then the elute is analysed with
2 ICPMS. The sulphide concentration in the AgI resin gel is directly analysed by computer-
3 imaging densitometry (CID). Using Fick's law, metal and sulphide concentrations in the
4 sediment pore waters are calculated and vertical profiles with a resolution of 5 mm for trace
5 metals [9, 10], but smaller for sulphide (here the resolution depends on the software that is
6 used) was obtained [11]. In addition, from those 1-D vertical solute profiles the exchange
7 fluxes at the water-sediment interface were estimated [3].

8 Most studies in anoxic sediments, involving trace metals and sulphide determinations by
9 the DGT technique, were limited to 1-D vertical profiles and a spatial resolution of 5 mm,
10 with the trace metals limiting this resolution [7, 8, 10, 11]. Recently, it became clear that
11 neither a spatial resolution of 5 mm, nor the limitation to 1-D profiles allow the detection of
12 microniches which are important features in anoxic sediments [12, 13]. In fact, in anoxic
13 sediments, burrow formation, irrigation, feeding and associated processes create distributions
14 of localized geochemical features, facilitating translocation of surface deposited material [13].
15 These localized small scale microniches are formed when discrete particles of reactive
16 organic matter are introduced at depth in the sediment. Their diameter can in principle vary
17 from a few microns up to the centimetre scale. Microniches give us information about the
18 geochemical processes occurring between the trace metals and sulphide, but with a low
19 resolution of a few mm many of the microniches remain invisible. Moreover, due to the
20 heterogeneity of the sediment, a 1-D profile cannot resolve their complete scale.

21 As yet mentioned above, increasing the spatial resolution and the extension from 1-D
22 profiling to 2D imaging for sulphide is only a question of improving the densitometry
23 software. For the trace metals, however, a new analysis technique is required. Indeed, the
24 classic resin-gel slicing technique has practical limitations for 2D imaging and for achieving
25 high resolution: a spatial resolution of smaller than a mm is a practical limit and even the
26 scale of mm is often not sufficient for understanding the sediment microstructure. Laser
27 Ablation - Inductively Coupled Plasma - Mass Spectrometry (LA-ICP-MS) can overcome
28 both limitations by offering a spatial resolution of about 100 μm in horizontal and vertical
29 dimensions, thus producing high resolution 2D images of the trace metal distribution in
30 anoxic sediments. Unfortunately, the Chelex-100 resin beads are too large for these
31 experiments, $\sim 100 \mu\text{m}$, and must be replaced by much smaller suspended particulate reagent-
32 iminodiacetate (SPR-IDA) resin beads (0.2 μm) [14].

33 The final challenge now is to combine the results of the trace metal profiles or images with
34 those of sulphide. In the past, 1-D profiles of metals with a relatively low resolution of 5 mm

1 were matched with high resolution 1-D profiles [15] or 2D images of sulphide suggesting
2 simultaneous remobilisation of both constituents [12]. However, these results were neither
3 derived from high resolution (sub mm scale) profiles, nor from superimposed 2D images,
4 implying that the uncertainty about the exact location of the increase in metal and sulphide
5 concentration is quite large. 2D imaging with a much higher spatial resolution (μm scale) and
6 the use of a single DGT probe for both trace metal and sulphide imaging is necessary to gain a
7 better understanding of local, small-scale remobilisation/precipitation zones.

8 We present here the first results of metal and sulphide mobilization in two dimensions in
9 highly polluted and organic rich sediments, using a new, combined DGT sampling probe (the
10 diffusive gel layer is formed by the AgI gel while the back-up layer is formed by the SPR-
11 IDA resin gel) and high resolution Laser Ablation ICP-MS (LA-ICP-MS) analysis, providing
12 superimposed 2D images of metals and sulphide at a resolution of about $100\ \mu\text{m}$.

13 **2. EXPERIMENTAL**

14 **2.1 Preparation of the SPR-IDA resin gel layer**

15 To prepare SPR-IDA resin gel, 1.25 mL gel solution (15% acrylamide, 0.3% DGT cross-
16 linker) was mixed with 1.25 mL of SPR-IDA resin ($0.2\ \mu\text{m}$ bead size). Sequentially, $17.5\ \mu\text{L}$
17 of 10% ammonium persulphate (APS, Merck) and $5.0\ \mu\text{L}$ tetramethylethylenediamine
18 (TEMED, >99%, Merck) were added and mixed well. Following mixing, the mixture was
19 immediately cast between glass plates separated by a $0.25\ \mu\text{m}$ plastic spacer, resulting in a 0.4
20 mm-thick resin gel after hydration. The resin gels were kept in 0.03 M NaCl (suprapur,
21 Merck) solution before their application.

22 **2.2 Preparation of the diffusive AgI gel layer**

23 In order to prepare AgI gel, 0.153 g of AgNO_3 (AnalaR, Merck) was dissolved in 0.45 mL
24 MilliQ water in a pre-cleaned polypropylene (PP) tube and 8.55 mL of gel solution (15%
25 acrylamide, 0.3% DGT cross-linker) was added and mixed well. Three mL of the mixture was
26 transferred to another PP tube and $10\ \mu\text{L}$ of 5% (w/w) APS (APS, >98%, Merck) was added
27 and mixed well. The gels were cast immediately between glass plates spaced by a $0.25\ \mu\text{m}$
28 plastic spacer, resulting in a 0.4 mm-thick gel after hydration. Following polymerization (45
29 minutes in the dark at room temperature), the glass plates were opened. The gel remained on
30 one plate, which was then immersed in a 0.2 M potassium iodide solution in a dark condition.
31 The gel became pale yellow within a few minutes and was peeled off from the glass plate.
32 Gels were kept in the KI solution overnight to allow full formation of the AgI gel.

1 Subsequently the AgI gels were washed several times in MilliQ water to remove the ions that
2 were adsorbed on the gel. The pH of the gel was also monitored and reached a value around 6
3 after rinsing. Then AgI gels were kept in 0.03 M NaCl (suprapur, Merck) solution before their
4 application.

5 **2.3 Preparation and application of the combined DGT probe**

6 To prepare the combined DGT probes in this study, the SPR-IDA resin gel was placed
7 behind an AgI gel, which was used as the diffusive gel. Motelica-Heino et al [12] compared
8 the diffusion rates of free metals in polyacrylamide (PA) and AgI gels deployed in metal
9 standard solutions and they found the same diffusion coefficients for both diffusive gels [12].

10 Since the resin is binding only free metals in solution, the contribution of metal-complexes
11 (ML) to the amount sequestered by the resin is a function of the ML dissociation kinetics in
12 the diffusive gel layer and at the resin interface. While the behaviour of most metal-
13 complexes will be the same in the classic polyacrylamide-chelex DGT as in the AgI-chelex
14 DGT, there could be a difference for metal-sulfide complexes. Silver reacts with free sulphide
15 and as a consequence it will compete and eventually dissociate metal-sulfide compounds that
16 are less stable than Ag₂S. This is not the case in the polyacrylamide diffusive gel layer.
17 Conditional stability constants corrected for side-reactions of the metal in seawater reported in
18 the literature [16] suggest that for example Fe(II), Mn(II) and Zn(II) sulphide complexes can
19 dissociate in the AgI gel layer while this is not the case for Cu(I) and Cu(II). Hence, for some
20 metals the AgI-chelex DGT result can be slightly higher than in the case of the classic DGT
21 involving a polyacrylamide gel layer, due to metal-sulfides that eventually dissociate in the
22 AgI gel layer. Further research must clarify the difference that may occur between
23 polyacrylamide and AgI gels with respect to metal-sulfide dissociation.

24

25 The AgI and SPR-IDA gels were overlain by a Millipore Durapore 0.45 µm filter
26 membrane (thickness 0.13 mm). All probes were deoxygenated prior to deployment by
27 purging N₂ for 24 h in 0.03 M NaCl (suprapur, Merck) solution. Sediment cores were
28 collected from the field allowing 5-10 cm overlying water to remain above the sediment. The
29 combined DGT probes were inserted into the sediment for several hours at field temperature
30 and in a dark room.

1 **2.4 Calibration procedure for trace metals and dissolved sulphide**

2 Combined DGT pistons were deployed in well-stirred 0.03 M NaCl solutions containing
3 five different concentration levels of Fe, Mn, Co, Cu and Ni, which were added as acidified
4 stock and metal salt standards (1000 mg L⁻¹), to give a final solution pH of 5. These
5 experimental conditions were necessary to avoid losses from the deployment solutions due to
6 adsorption to the container walls and from the formation of colloidal species. Every hour sub-
7 samples (1 ml) were taken from the bulk solution, acidified and analysed by ICPMS. Four
8 DGT pistons were removed from each of the deployment solutions after 5h. One of the resin
9 gel standards was immediately transferred onto new acid-washed 0.45- μ m cellulose nitrate
10 filters, similar to those that were used in the deployment, and dried using a commercial gel
11 dryer (BioRad, Germany) at 60 °C for 24 h according to the procedure presented by Warnken
12 et al. [14]. Once dried, these gel standards were cut into a suitable size and then mounted on a
13 glass plate, using double sided tape, for Laser Ablation ICPMS analysis (Thermo Elemental
14 X-SeriesII ICPMS connected to an ESI 193FX laser ablation system). Three of the above
15 resin gel standards were eluted with 1 mL of 1 mol L⁻¹ HNO₃ and analysed with ICPMS
16 against certified solution standards to quantify the mass of metal present on the resin gel. The
17 laser ablation data was plotted as the normalized metal count rate (metal count rate divided by
18 the internal standard ¹³C-count rate) versus the amount of metal determined per unit area of
19 resin gel (nmol cm⁻²).

20 A sulphide stock solution of 1,000 mg L⁻¹, was prepared from Na₂S.9H₂O (>98%, Sigma
21 Aldrich, USA) in a deoxygenated borate buffer (pH = 8.2) and stored in a refrigerator. The
22 sulphide standard solutions of 5 to 100 μ mol L⁻¹ were prepared in brown glass bottles by
23 diluting the sulphide stock solution in 500 mL of deoxygenated borate buffer solution (pH =
24 8.2). Three combined DGT pistons were deployed in the standard solution for 4 hours under
25 oxygen free condition. The AgI gels were peeled off from the piston after the deployment and
26 the colour change from pale yellow to black, due to the formation of silver sulphide at various
27 concentrations, was scanned by a flat-bed scanner (HP 3100). ImageJ software allows
28 measurement of average optical density for a chosen area. The optical density for AgI gel
29 deployed in sulphide standard solutions was plotted as greyscale density versus the amount of
30 sulphide determined per unit area of AgI gel (nmol cm⁻²).

31 To make sure the sulphide concentrations remained stable during the deployment, sub-
32 samples of the sulphide solutions were taken before and after the experiment. These solutions
33 were checked with methylene blue method [17]. The first mixed diamine reagent was

1 prepared by dissolving 2.0 g of N,N-dimethyl-p-phenylenediamine oxalate (ICN Bio-
2 chemicals, USA) and 3.0 g of FeCl₃ (P.A. >99%, Merck, Germany) in 500 mL of 30 % HCl
3 acid (Suprapur 30%, Merck, Germany). The second mixed diamine reagent was prepared by
4 dissolving 8.0 g of the oxalate and 12.0 g of the FeCl₃ in 500 mL of 30 % HCl acid. The first
5 one was used for the 5, 10 and 20 μmol L⁻¹ solution (1:1 ratio) and the second one for the 50
6 and 100 μmol L⁻¹ solution (also 1:1 ratio). The absorbance (A) of the sulphide solutions was
7 measured at a wavelength of 670 nm with a UV-vis spectrometer (Spectronic Genesys 5,
8 Thermo Electron, USA).

9 **2.5 Retrieval and Analysis of the AgI and SPR-IDA gels**

10 After the deployment of the combined DGTs in sediment cores, the SPR-IDA and AgI gels
11 were peeled from the combined DGT probes and the SPR-IDA gels were dried onto a
12 Durapore filter at 60°C for 24 hours using the gel drier. Analysis of trace metals at 100 μm
13 spatial resolution was performed by LA-ICP-MS using a line scan mode procedure [15].
14 Briefly a 100 μm diameter beam was scanned across the gels in a series of lines (100 μm
15 apart) at 50 μm s⁻¹. C13 was used as an internal standard. The laser data obtained for trace
16 metals in gel samples were transformed into concentration based on the calibration curves.
17 For sulphide analysis, the AgI gels were scanned by a flat-bed scanner to provide a grey-scale
18 image of sulphide. Image processing software ImageJ and SigmaPlot were used to convert the
19 scanned images into 2D images of sulphide concentration with a resolution of 85 μm based on
20 the sulphide calibration curve.

21 **3. RESULTS AND DISCUSSION**

22 **3.1 Calibration and validation**

23 Trace metal calibration curves were established with 5 different trace metal standards: the
24 LA-ICP-MS signal (number of counts) was plotted against the mass of trace metal on the
25 resin (nmol cm⁻²). Each of the 5 standards is the average of the results obtained on 3 replicate
26 resin gels deployed in the same metal concentration solution. These replicates show in general
27 a RSD (relative standard deviation) around 5%. The fourth resin gel deployed in the same
28 metal concentration solution is analysed by LA-ICP-MS using a line scan mode procedure
29 [18]. Mandel's fitting test was used to check the regression of these calibration curves. Linear
30 regression was preferred over quadratic for trace metals. The regression coefficient for Fe,
31 Mn, Co, Cu and Ni was 0.994, 0.987, 0.992, 0.974 and 0.997, respectively.

1 Detection limits (LOD's) of Fe, Mn, Co, Cu and Ni concentrations in the SPR-IDA resin
2 were respectively 0.23, 0.33, 0.0039, 0.060 and 0.10 nmol.cm⁻². The method was sensitive
3 enough because all our field results were above these LODs. Repeatability for these metals
4 was below the Horwitz threshold [19] of 14.7%, whilst reproducibility was below the
5 threshold of 22%.

6 Sulphide calibration curve, where the optical density (OD) was plotted as greyscale density
7 versus the amount of sulphide determined per unit area of AgI gel (nmol.cm⁻²), were
8 established with 5 different sulphide standard concentrations (Fig 1). The sulphide standard
9 concentrations (5, 10, 20, 50 and 100 μmol L⁻¹) were checked before and after use with the
10 methylene blue method [17]. To calibrate the pixel density as function of the sulphide
11 concentration (nmol cm⁻²), a non-linear regression was used. A hyperbolic function gave the
12 best fit, with p-values for all coefficients lower than 0.05 for the 95% confidence interval,
13 which means that our coefficients are very likely. The LOD of the sulphide analysis method
14 was 6.5 nmol cm⁻². The method is sensitive enough to determine sulphide in the pore waters
15 of our estuarine and marine sediments. The calibration equation was as follows:

$$16 \quad y = y_0 + (a * x) / (b + x)$$

17 where $y_0 = (46.2 + 4.0)$, $a = (173.0 + 9.0)$ and $b = (870 + 150)$ nmol.cm⁻².

18 Different studies compared the sulphide results obtained by the AgI-DGT method with
19 other analytical methods. A procedure for measuring in situ sulphide concentrations by
20 coupling diffusive gradients in thin films (DGT) to solid state ion-selective electrodes (ISE)
21 was compared to computer imaging densitometry (CID) and methylene blue method [20].
22 Regressions of the sulphide mass accumulation versus the independent variables of time and
23 inverse diffusive thickness proved to be linear. All performance tests of the DGT-ISE method
24 compared favourably with previous results that were generated by DGT probes coupled to
25 methylene blue and densitometric measurements. Also Lesven [21] measured sulphide pore
26 water profiles in sediments of the Espierre River, northern France, with different analytical
27 methods. The results obtained with AgI-DGT, voltammetry and methylene blue method
28 compared well [21].

29 **3.2 Sediment pore water fluxes and concentrations**

30 When a sustained ion flux from pore water to the DGT resin exists, it is possible to
31 calculate the ion concentration in the pore water by using Fick's diffusion law and the mass of
32 ion determined in the resin gel.

$$33 \quad Cdgt = (M * \Delta g) / (D * t * A)$$

1 where C_{dgt} is DGT measured concentration; M is mass of metals, which is obtained by LA-
2 ICP-MS analysis; Δg is thickness of diffusive gel; D is the diffusive coefficient of solute in
3 diffusive gel; A is the surface of the gel exposed to the bulk solution and t is deployment time.
4 In case of sustained supply we can express the results in concentrations instead of fluxes,
5 which is the case in our sediments [22].

6 **3.3 Estuarine sediments**

7 The Zenne River in Belgium receives high loads of organic material, pollutants like trace
8 metals and micro-organic pollutants that partly accumulate in the sediments. DGT Fe
9 concentration increased steadily from the sediment water interface (SWI) and reached a
10 maximum concentration around -0.5 cm (Fig. 2). In this narrow zone the concentration ranges
11 from 5 μM to 25 μM , but below this zone and down to 6 cm, a constant Fe concentration level
12 of around 10 μM prevailed. The sulphide concentration started to increase immediately below
13 the SWI, achieving a maximum value of 7 μM at -0.1 cm of depth, a few mm above the Fe
14 production zone (Fig 3). The reduction of sulphate happens very close to the reduction zone
15 of Fe^{3+} , but dominates it, leading to FeS precipitation.

16 Lower in the sediments, a sulphide hotspot was found with a maximum concentration of 6
17 μM at around -4.1 to -4.6 cm (Fig 3). This hotspot was superimposed on a relatively constant
18 background of 2 to 3 μM . None of the metals investigated showed elevated concentrations at
19 the same location as the sulphide hotspot, indicating that they were not simultaneously
20 released with the sulphide.

21 **3.4 Marine sediments**

22 Sulfide hotspot formation

23 The Belgian coastal zone (BCZ) is strongly influenced by eutrophic rivers such as Scheldt,
24 Rhine and Meuse resulting in phytoplankton blooms. Spring blooms begin in March when
25 nutrient, light and temperature conditions become sufficient for phytoplankton growth and
26 terminate in April-May with the onset of nutrient limitation, after which large amounts of
27 organic material sediment out [23, 24]. As a consequence, the degradation of increasing
28 amounts of freshly deposited organic matter changes the physicochemical conditions in the
29 sediment interface potentially releasing trace metals from the sediments into the water column
30 [7, 25].

31 The dissolved sulphide profiles showed 2 zones of elevated levels: zone 1 (SWI to - 1 cm
32 of depth) and zone 2 (- 5 cm of depth to the bottom of the DGT probe). At the SWI the
33 sulphide concentration was around 2 μM and then dropped gradually to 1 μM . In the

1 intermediate zone (between - 1 and - 5 cm of depth) the sulphide concentration remained at 1
2 μM (Fig. 4a). Metals showed a different pattern from that of dissolved sulphide. The
3 concentrations of Fe, Mn and Co increased as soon as the sulphide concentration decreased to
4 a value of 1 μM (Fig 4b, 4c, 4d). This trend of decreasing sulphide concomitantly with
5 increasing trace metals reflects the classic relationship between them.

6 Dissolved sulphide concentrations in zone 2 (-5 cm to the bottom of the DGT probe) are
7 again high with concentrations ranging from 2 μM to 14 μM , indicating that the sediments
8 were completely anoxic with sulphate reduction occurring. The consequence of this sulphide
9 production was metal precipitation, so that the metal concentrations were low (Fig 5).

10 Simultaneous remobilisation of sulphide and metals:

11 In marine sediments, the sulphide concentrations are much higher than estuarine sediment
12 which means that if there is a hotspot it will be superimposed on a high sulphide background,
13 making it harder to detect. The AgI gel showed a rather broad zone of aggregated hotspots at a
14 depth of -10 to -12 cm in the deeper sediment layer (Fig 6). At a depth of -11.10 to -11.80 cm,
15 Fe, Mn, Co and Ni were released at the same location inside a much larger sulphide hotspot
16 area (Fig 7). The dissolved sulphide concentration increased from -10.8 cm and reached a
17 maximum concentration of around 55 μM at -11.17 cm. This generally high level of sulphide
18 extended to a depth of -11.40 cm. Inside the sulphide elevation zone (7 mm of length), Co and
19 Ni had single sharp maxima at a depth of -11.17 cm with concentrations of 0.12 μM and 0.42
20 μM , respectively (Fig 7). Fe and Mn also reached their highest concentration values of 33 μM
21 and 2.6 μM at this depth, but they also had several smaller maxima at slightly greater depths.
22 The shape of the sulphide hotspots was like a “butterfly” with the remobilisation of metals
23 appearing on the left wing area, but with no release of metals corresponding to the right wing
24 area, even though the sulphide concentration there was higher (Fig 6). The remobilisation of
25 metals probably only happened in a few small niches of the agglomerated overall hotspot.
26 Visual Minteq software was used to calculate the saturation index of FeS, MnS, CoS and NiS
27 minerals at -11.17 cm of depth. The calculation showed that there was super-saturation for
28 FeS, CoS and NiS at that location, but not for MnS.

29 **4. CONCLUSION**

30 To investigate the prevalence of simultaneous remobilisation of sulphide and trace metals
31 in aquatic sediments a novel method, combining a DGT probe consisting of a SPR-IDA
32 micro-chelex resin with an AgI diffusive gel and a LA-ICP-MS measuring technique, was
33 used. Very low concentrations of sulphide and trace metals can be determined in the pore

1 waters because the passive DGT sampler can be deployed for long term meanwhile
2 accumulating these ions. In addition, since the gel layers for sulphide and trace metals are
3 superimposed, an elevated concentration of a trace metal can be exactly positioned versus a
4 sulphide hotspot.

5 The low RSDs on replicate measurements, the linearity of the trace metal calibration
6 curves and the good agreement of the sulphide results obtained with different analytical
7 methods are indicators of the validity of the analytical procedures. Since the scale of sulphide
8 and trace metal remobilisation in anoxic sediments is very small (down to sub-mm level),
9 high resolution imaging is necessary. With the LA-ICP-MS and densitometric scanning
10 procedures, a resolution of the order of 100 μm is routinely achievable. The application of the
11 novel method allowed observing, for the first time, 2D-images of simultaneous metals and
12 sulphide remobilisation in marine sediments. In Zenne sediments, no simultaneous
13 remobilisation of sulphide and metals was detected.

14 As the background concentration of sulphide is much higher in marine than in estuarine
15 sediments (about a factor of 10), it is commonly more difficult to distinguish in the marine
16 environment hotspots of sulphide release. However, in the pore waters of the marine
17 sediments we observed two distinctive geochemical phenomena; the progressive release of
18 low concentrations of sulphide in the sub-surface layer coupled with isolated hotspots in the
19 deeper layers. The former observation is consistent with the activity of Desulfoculbaceae
20 bacteria, which are known to be prevalent in the Belgian Coastal Zone [26]. Consuming
21 dissolved sulphide these strictly anaerobic, filamentous bacteria act as electrical cells passing
22 electrons generated by sulphide oxidation to the upper sediment layer where they are
23 consumed by oxygen reduction [27]. Preliminary results from laboratory experiments indicate
24 that the activity of these bacteria induces strong pH gradients.

25 Coincident remobilisation of sulphide and metals in microniches zones of heightened
26 sulphide release, as evidenced in the marine sediments below -11 cm can be explained by the
27 supersaturation of metal sulphide; a process driven by electron dispensing, highly reactive
28 organic parcels [12].

29 This study shows the first measurements of simultaneous trace metals and sulphide release
30 in marine sediments and contrasts directly with the conventional view of sediments that
31 dissolved metal concentrations are very low in the presence of elevated sulphide. The
32 importance of this overlooked mechanism of metal release requires further study, in particular
33 future work should target environments where either filament bacteria or reactive organic

1 parcels are present. The method we presented in this paper constitutes an essential element for
2 the performance of such studies.

3 **5. ACKNOWLEDGEMENTS**

4 Yue Gao thanks FWO for a postdoc fellowship. The authors are also grateful to André
5 Cattrijsse and the crew of RV Simon Stevin.

6 **References**

- 7 1. D. M. Di Toro, J. D. Mahony, D. J. Hansen, K. J. Scott, M. B. Hicks, S. M. Mayr, M.
8 S. Redmond, Toxicity of cadmium in sediments: the role of acid volatile sulfide.
9 *Environ. Toxicol. Chem.* 9 (1990) 1487.
- 10 2. G. T. Ankley, G. L. Phipps, E. N. Leonard, D. A. Benoit, V. R. Mattson, P. A.
11 Kosian, A. M. Cotter, J. R. Dierkes, D. J. Hansen, J. D. Mahony, Acid volatile
12 sulphide as a factor mediating cadmium and nickel bioavailability in contaminated
13 sediments. *Environ. Toxicol. Chem.* 10 (1991) 1299.
- 14 3. Y. Gao, L. Lesven, D. Gillan, K. Sabbe, G. Billon, S. De Galan, M. Elskens,
15 Baeyens, W. Leermakers, M. Geochemical behavior of trace elements in sub-tidal
16 marine sediments of the Belgian coast, *Mar. Chem.* 117 (2009) 88–96.
- 17 4. Y. Gao, M. Leermakers, A. Pede, A. Magnier, K. Sabbe, B. Lourino Cabana, G.
18 Billon, W. Baeyens, D. C. Gillan, Response of DET and DGT trace metal profiles in
19 sediments to phytodetritus mineralization, *Environ. Chem.* 9 (2012) 41-47.
- 20 5. S. Panutrakul, W. Baeyens, Behavior of heavy-metals in mud flat of the Scheldt
21 estuary, Belgium. *Mar. Pollut. Bull.* 22 (1991), 128-134.
- 22 6. G. Billon, B. Ouddane, P. Recourt, A. Boughriet, Depth variability and some
23 geochemical characteristics of Fe, Mn, Ca, Mg, Sr, S, P Cd and Zn in anoxic
24 sediments from Authie Bay (Northern France), *Estuar. Coast. Shelf Sci.* 55 (2002),
25 167-181.
- 26 7. Y. Gao, M. Leermakers, C. Gabelle, M. Wartel, G. Billon, B. Ouddane, J. C.
27 Fischer, W. Baeyens, High Resolution Profiles of Trace Metals in the Pore Waters of
28 Riverine Sediment Assessed by DET and DGT, *Sci. Total Environ.* 362 (2006) 266-
29 277.
- 30 8. Y. Gao, M. Leermakers, M. Elskens, G. Billon, B. Ouddane, J. C. Fischer, W.
31 Baeyens, High Resolution Profiles of Thallium, Manganese and Iron Assessed by
32 DET and DGT Techniques in Riverine Sediment Pore Waters, *Sci. Total Environ.* 373
33 (2007) 526-533.
- 34 9. W. Davison, H. Zhang, In situ speciation measurements of trace components in
35 natural waters using thin-film gels, *Nature.* 367 (1994) 546–548.
- 36 10. H. Zhang, W. Davison, R. J.G. Mortimer, M. D. Krom, P. J. Hayes, I. M. Davies,
37 Localised remobilization of metals in a marine sediment, *Sci. Total Environ.* 296
38 (2002) 175–187.

- 1 11. P. R. Teasdale, S. Hayward, W. Davison, In situ, High-Resolution Measurement
2 of Dissolved Sulphide Using Diffusive Gradients in Thin Films with Computer-Imaging
3 Densitometry, *Anal. Chem.* 71 (1999) 2186-2191.
- 4 12. M. Motelica-Heino, C. Naylor, H. Zhang, W. Davison, Simultaneous Release of
5 Metals and Sulphide in Lacustrine Sediment, *Environ. Sci. Technol.* 37 (2003) 4374-
6 4381.
- 7 13. A. Stockdale, W. Davison, H. Zhang, Micro-scale biogeochemical heterogeneity
8 in sediments: A review of available technology and observed evidence, *Earth Sci.*
9 *Res. J.* (2009) 81–97.
- 10 14. K. W. Warnken, H. Zhang, W. Davison, Performance characteristics of
11 suspended particulate reagent-iminodiacetate as a binding agent for diffusive
12 gradients in thin films, *Anal. Chim. Acta.* 508 (2004a) 41–51.
- 13 15. C. Naylor, W. Davison, M. Motelica-Heino, G. A. Van Den Berg, M. L. Van Der
14 Heijdt, Simultaneous release of sulphide with Fe, Mn, Ni and Zn in marine harbour
15 sediment measured using a combined metal/sulphide DGT probe, *Sci. Total Environ.*
16 328 (2004) 275–286.
- 17 16. R. Al-Farawati, C. M. G. van den Berg, Metal-sulfide complexation in seawater,
18 *Mar. Chem.* (1999) 331-352.
- 19 17. J. D. Cline, Spectrophotometric determination of hydrogen sulphide in natural
20 waters, *Limnol. Oceanogr.* 14 (1969) 454-58.
- 21 18. Y. Gao, N. Letho, A simple laser ablation ICPMS method for the determination of
22 trace metals in a resin gel, *Talanta.* 92 (2012) 78– 83.
- 23 19. M. Thompson, Recent trends in inter-laboratory precision at ppb and sub-ppb
24 concentrations in relating to fitness for purpose criteria in proficiency testing, *Analyst.*
25 125 (2000) 385-386.
- 26 20. S. Rearick, C. C. Gilmour, A. Heyes, R. P. MASON, Measuring sulphide
27 accumulation in diffusive gradients in thin films by means of purge and trap followed
28 by ion-selective electrode, *Environ. Toxicol. Chem.* 24 (2005) 3043-3047.
- 29 21. L. Lesven, Fate of trace metals in sediment, a key compartment of the aquatic
30 environment (translated from the French title), PhD thesis. Defended on 02112/2008.
- 31 22. B. Lourino-Cabana, G. Billon, L. Lesven, K. Sabbe, D. C. Gillan, Y. Gao, M.
32 Leermakers, W. Baeyens, Monthly variation of trace metals in North Sea sediments.
33 From experimental data to modeling calculations, *Mar. Pollut. Bull.*, in press (2014).
- 34 23. V. Rousseau, S. Bequevort, J. Y. Parent, S. Gasparini, M. H. Daro, M. Tackx, C.
35 Lancelot, Trophic efficiency of the planktonic food web in a coastal ecosystem
36 dominated by *Phaeocystis* colonies, *J. Sea Res.* 43 (2004) 357–372.
- 37 24. K. Muylaert, R. Gonzales, M. Franck, M. Lionard, C. Van der Zee, A. Cattrijsse,
38 K. Sabbe, L. Chou, W. Vyverman, Spatial variation in phytoplankton dynamics in the
39 Belgian coastal zone of the North Sea studied by microscopy, HPLC-CHEMTAX and
40 underway fluorescence recordings, *J. Sea Res.* 55 (2006) 253–265.
- 41 25. S.T. Pakhomova, P.O.J. Hall, M.Y. Kononets, A.G. Rozanov, A. Tengberg, A.V.
42 Vershinin, Fluxes of iron and manganese across the sediment–water interface under
43 various redox conditions, *Mar. Chem.* 107 (2007) 319–331.

- 1 26. S. Y. Malkin, A. M. F. Rao, D. Seitaj, D. Vasquez-Cardenas, E. M. Zetsche, H. T.
2 S. Boschker, F. J. R. Meysman, Natural occurrence of microbial sulphur oxidation by
3 long-range electron transport in the seafloor, ISME J. in press (2014).
- 4 27. C. Pfeffer, S. Larsen, J. Song, M. D. Dong, F. Besenbacher, R. L. Meyer, K. U.
5 Kjeldsen, L. Schreiber, Y. A. Gorby, M. Y. El-Naggar, K. M. Leung, A. Schramm, N.
6 Risgaard-Petersen, L. P. Nielsen, Filamentous bacteria transport electrons over
7 centimetre distances, Nature. 49 (2012) 219-221.
- 8

1 **Figure legend and figures**

2 Figure 1 Plot of greyscale density (0-255) versus sulphide per cm² for 5 sulphide standards
3 and the black line is the fitted calibration curve.

4

5 Figure 2 2D image of Fe at the Sediment Water Interface (SWI) of an estuarine sediment

6

7 Figure 3 (a) Greyscale image of AgI gel deployed in an estuarine sediment; (b) 1D vertical
8 profile of sulphide concentration; (c) 2D image of sulphide at the SWI of an estuarine
9 sediment; (d) 2D image of a sulphide hotspot

10

11 Figure 4 2D images of sulphide, Fe, Mn and Co at the SWI of a marine sediment

12

13 Figure 5 2D images of sulphide and Fe (zone 2, below 4.5 cm of depth) in a marine sediment

14

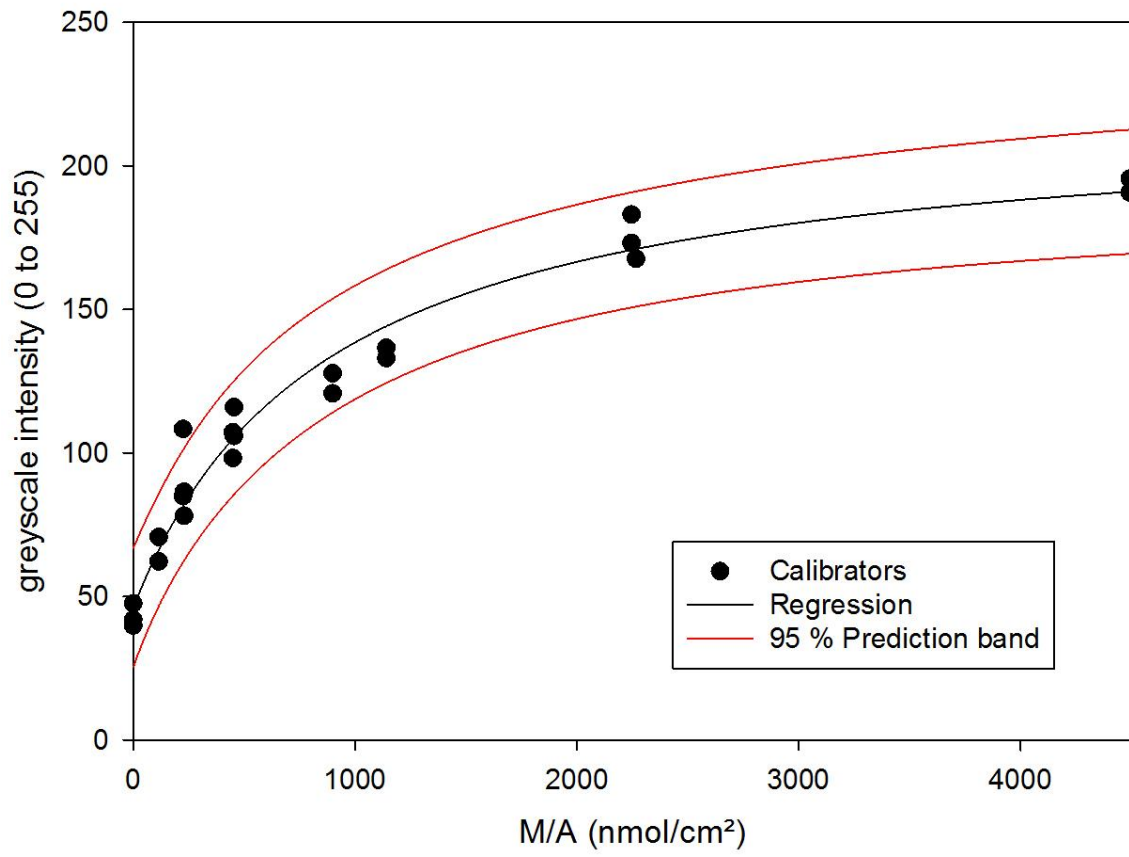
15 Figure 6 (a) Greyscale image of AgI gel deployed in a marine sediment; (b) 2D contour figure
16 drawing of sulphide hotspots in a marine sediment; (c) the corresponding 2D contour figure
17 drawing of Fe hotspots

18

19 Figure 7 1D vertical profiles of Fe, Mn, Co and Ni concentrations a marine sediment

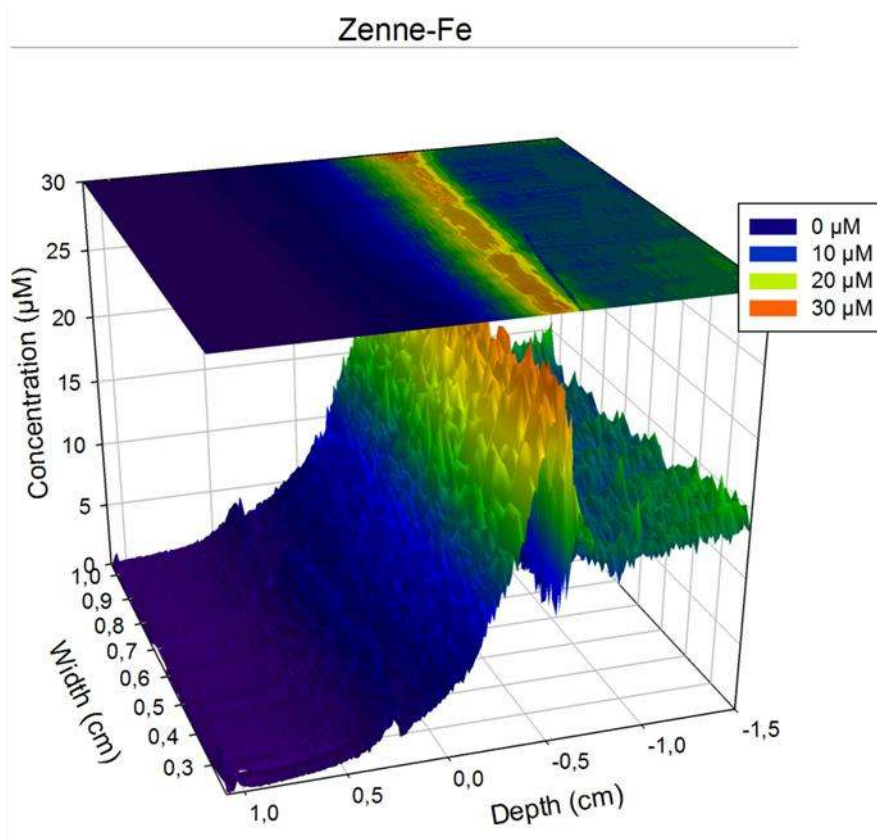
20

1 **Figure 1:**



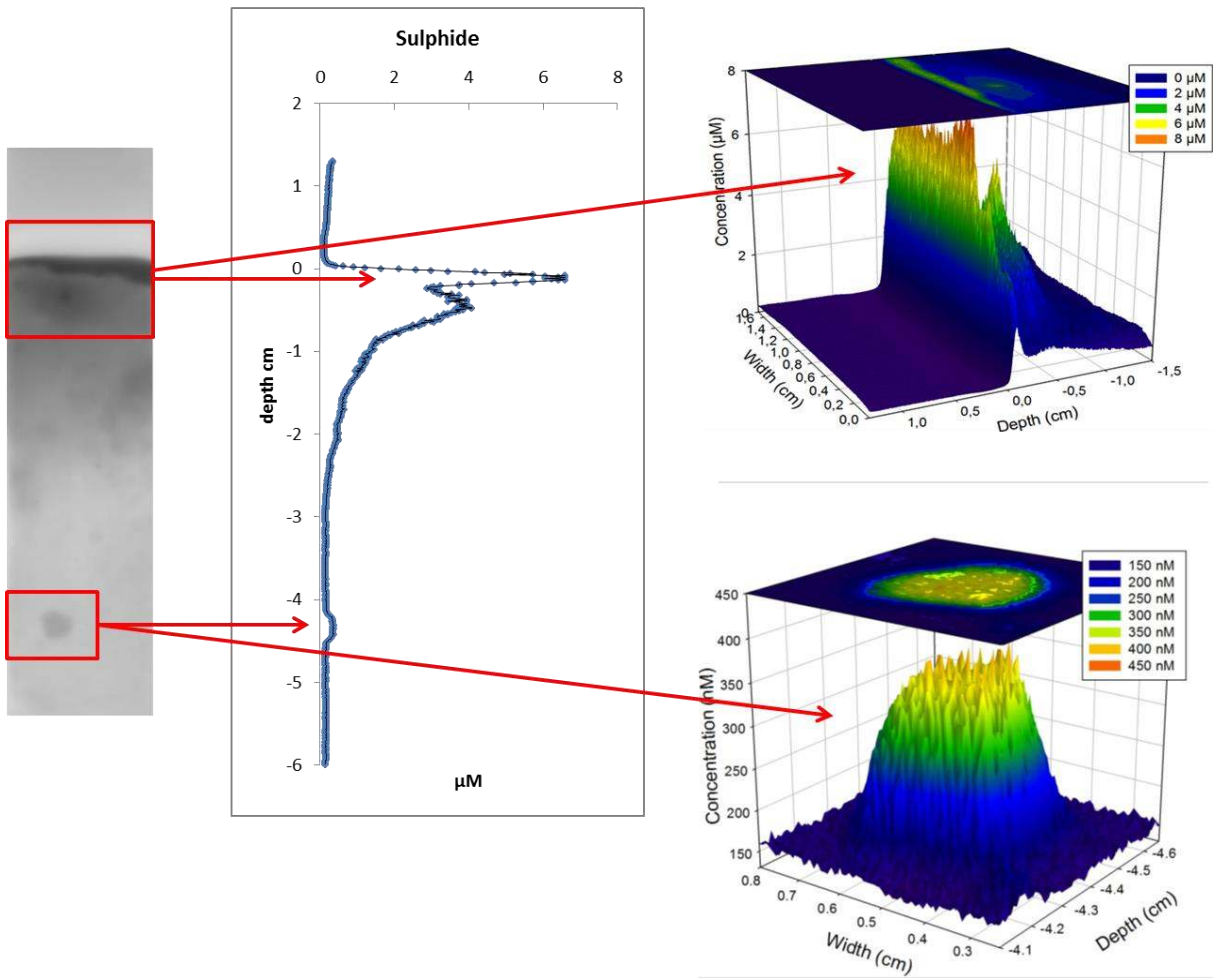
2
3

1 **Figure 2:**
2



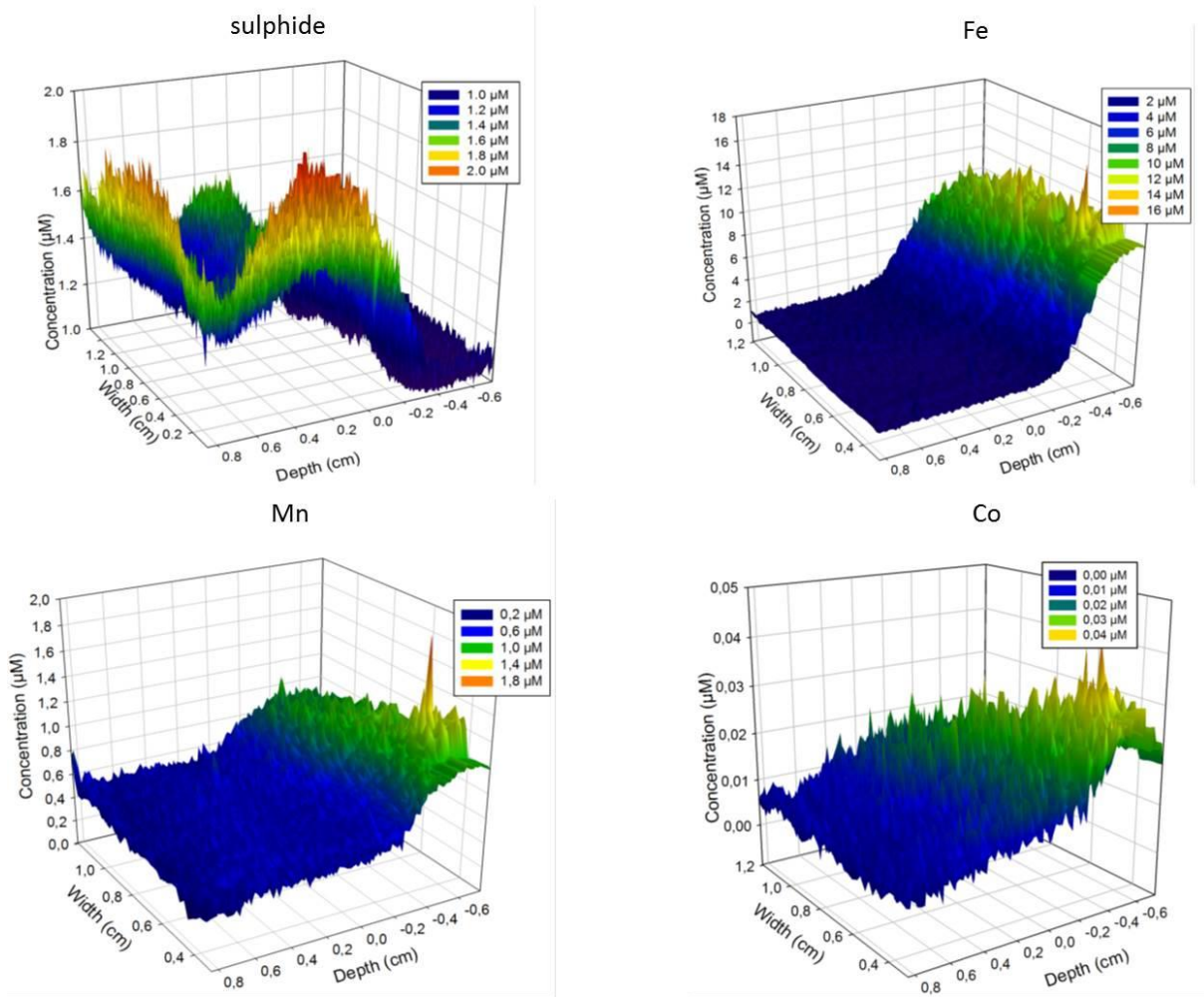
3
4

1 **Figure 3:**
2



3
4

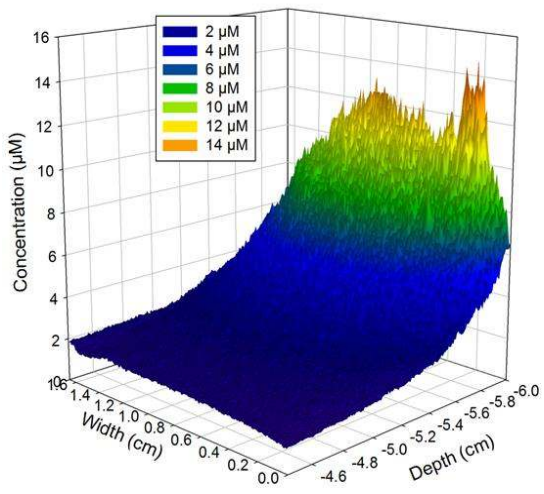
1 **Figure 4:**
2



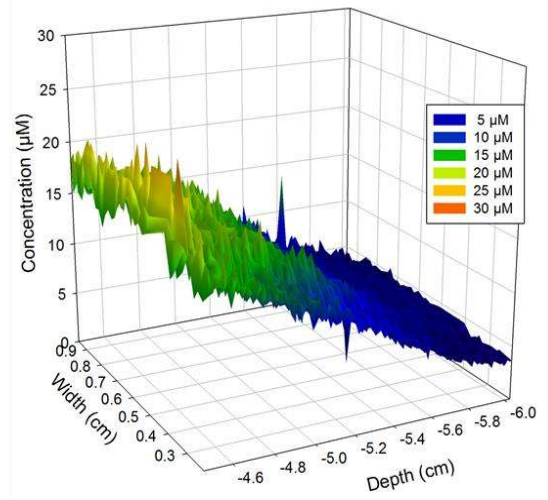
3
4

1 **Figure 5:**

2



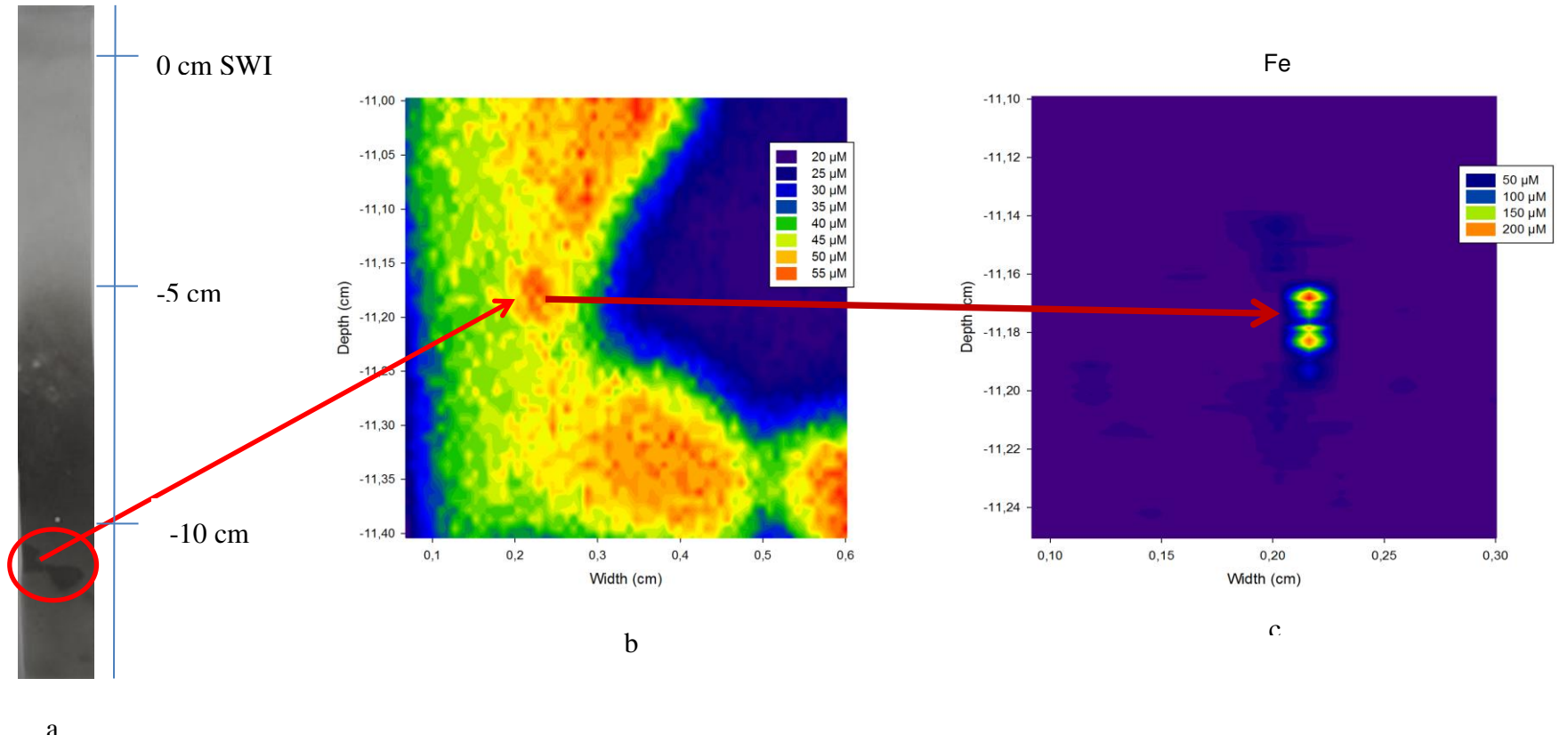
3



1 **Figure 6:**

2

3



1 **Figure 7:**

2

